

Boron in amorphous silicon: an *ab initio* study

Iván Santos,^{1,2,*} Wolfgang Windl,^{1,†} D. A. Drabold,³ Lourdes Pelaz,² and Luis A. Marqués²

¹*Department of Materials Science and Engineering, The Ohio State University,
2041 College Road, Columbus, OH 43210-1178, USA*

²*Departamento de Electricidad y Electrónica, Universidad de Valladolid,
E.T.S.I. de Telecomunicación, 47011 Valladolid, Spain*

³*Department of Physics and Astronomy,
Ohio University, Athens, Ohio 45701-2979, USA*

(Dated: March 2, 2009)

Abstract

We have performed an *ab initio* study of B in amorphous Si by analyzing different substitutional- (a Si atom in the amorphous cell is replaced by a B atom, B_s) and interstitial-like (a B atom is added into an interstitial space, B_i) configurations. We find substitutional-like B (B_s and B_i that relaxes to four-fold coordination) with negative charge to have the lowest chemical potential at mid-gap, with a linear scaling of the B_s chemical potential with the average nearest-neighbor distance. The negative charge-state confirms the unexpected (but experimentally observed) capability of doping amorphous Si. Non-fourfold B_i atoms have an averaged formation energy of 1.5 eV at mid-gap. A molecular dynamics study with subsequent nudged-elastic band optimization results in a migration barrier of ~ 0.6 eV and an activation energy of 2.1 eV which is in the experimental range.

PACS numbers: 31.15.A-, 81.05.Gc, 85.40.Ry

Boron is the dominant p -type dopant in silicon. It has been extensively studied in crystalline Si (c -Si), and diffusion [1–3], interaction with Si atoms [4] and segregation processes [5–7] are well known. It is well established that the location of B atoms in the the crystalline lattice, i.e. interstitial or substitutional positions, determines their capability to diffuse and their electrical activity. According to the last edition of the International Technology Roadmap for Semiconductors [10], future device generations will require a more precise control of the doping of electrically active regions in order to continue the scaling-down of the device dimensions. Solid-phase epitaxial regrowth (SPER) of doped a -Si at temperatures of 600 – 700°C has been proposed as a candidate for fabricating state-of-the-art Si devices since it enables high active dopant concentrations with minimal diffusion [10]. In addition, amorphous semiconductors are the material of choice in many other applications: solar cells, optical sensors, microbolometers, memory elements, etc. Consequently, a good knowledge of dopant behavior in this type of materials is required in order to understand the underlying physics and thus optimize processing and materials performance in many different applications. However, only little work at the atomic level exists for B in amorphous Si (a -Si) [8, 9]. Computer simulation techniques represent a powerful tool to obtain useful information at the atomic level typically not available from experiments.

The aim of this work is to understand the energetics and environment of B atoms in a -Si. Due to the underlying amorphous network, there will be a continuous range of configurations rather than the discrete set of a crystalline environment. The dynamical features of B in a -Si might be formulated as hopping between various metastable configurations in this energy landscape. In contrast to the crystal, the a -Si network has a higher probability of rearranging, changing the energy landscape during annealing, and therefore influencing the diffusion process.

We have carried out an *ab initio* study of B in a 64-atom a -Si cell. One of the most used computer models of a -Si is the one proposed by Wooten, Weaire and Winer [11] (WWW), which is based on a particular bond-switching algorithm and extremely simple potentials. However, in this work we use a model developed by Barkema and Mousseau [12, 13] (BM), who proposed an algorithm significantly improved over the original WWW scheme. The BM model uses a random initial configuration which guarantees that there is no ‘crystalline remnant’, a drawback of early models. Upon relaxing with *ab initio* interactions, the BM structure barely changes at all. To represent the amorphous environment faithfully, it is

necessary to work with cells of at least several hundred atoms, and it is desirable to have even more. The difficulty with smaller models is that there are discernible strain effects (most notable in a slightly broadened bond angle distribution relative to experiment). Nevertheless, for local structural and electronic properties as we are focused on here, we anticipate that the strain artifacts will not be large. As discussed below, the cell used properly includes the correct local topological disorder of the material, and is big enough for a high-precision calculation that includes B.

For our *ab initio* calculations, we have used the density-functional theory code VASP [14] with generalized gradient approximation ultrasoft pseudopotentials [15]. The energy cutoff chosen was 230 eV. We used a $4 \times 4 \times 4$ Monkhorst-Pack k-point mesh for density of states (DOS) calculations, and $2 \times 2 \times 2$ k-points for cell relaxations. For molecular dynamics (MD) simulations, we used an energy cutoff of 156 eV and Γ -point sampling. We considered two different sets of initial configurations for B atoms: substitutional-like (B_s) and interstitial-like (B_i) ones. For the former, we replaced one of the Si atoms of the cell by a B atom. For the latter, we added a B atom in an interstitial site. Subsequently, we carried out relaxations of both the atomic positions and cell shape and volume in order to find the nearest local minimum configurations. Among other effects, this causes rearrangement events of Si atoms around B, which however are a consequence of the initial relaxation and do not constitute diffusion events. In the resulting structures, all relaxed B_s atoms were fourfold coordinated. For B_i atoms, we found interstitial B with threefold [$B_i(3)$], fourfold [$B_i(4)$] and fivefold [$B_i(5)$] coordination. We have considered all 64 substitutional and additionally 142 interstitial configurations. We would like to point out that we do not use “substitutional” and “interstitial” in the narrow sense these terms are used for crystalline materials, but more generally to distinguish how the B atoms were inserted into the cell.

We first evaluated the band gap of the undoped *a*-Si sample by means of a density of states calculation. In the case of *c*-Si, *ab initio* DFT calculations give a value of 0.63 eV [16] instead of the experimental 1.12 eV (at 300 K) [17]. Nevertheless, scissor, finite-size, and gap-state corrections have been proposed for such calculations [16]. In the case of the *a*-Si sample considered, we obtained from the DOS calculation a gap value of 0.76 eV, which is 21% larger than the theoretical value. However, gap corrections in *a*-Si are much more difficult since there is not a unique reference. As a first approximation, we can estimate the corrected gap value in *a*-Si to be 21% larger than the experimental value for *c*-Si. This

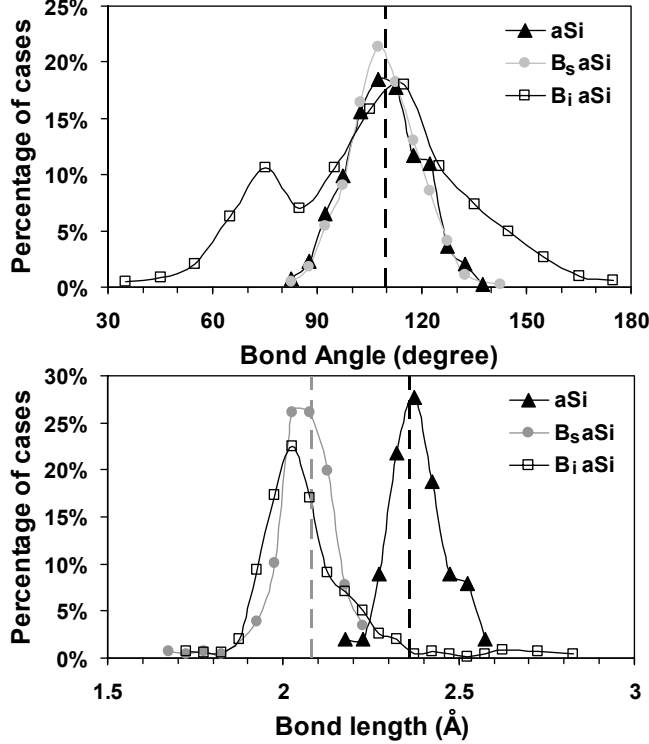


FIG. 1: Bond angle and bond length distributions for Si, B_s, and B_i atoms in *a*-Si. The corresponding values for Si and B_s atoms in *c*-Si are given by black and gray dashed lines respectively.

gives a gap value of 1.36 eV for *a*-Si, which is in agreement with previously reported values [13, 18, 19].

Next, we characterized both the *a*-Si cell and the environment of the B atoms. In Fig. 1 we represent the distributions of bond lengths and angles for Si, B_s, and B_i atoms in *a*-Si. For that purpose we have defined a nearest-neighbor coordination using a cutoff of 2.85 Å. This cutoff lies in the middle of the empty region between the first and the second peaks of the pair correlation function of the relaxed *a*-Si sample. With this cutoff, all Si atoms are fourfold coordinated in the undoped sample. Their average bond length and angle are 2.37 ± 0.08 Å and $109.13 \pm 10.45^\circ$, while the corresponding values in *c*-Si are 2.36 Å and 109.47° . Regarding B_s atoms, their average bond lengths and angles are 2.08 Å and 109.47° in *c*-Si and 2.07 ± 0.06 Å and $109.21 \pm 9.54^\circ$ in *a*-Si, which is 12% and 13% shorter than the Si-Si bond length of their respective cells. Furthermore, angle distribution for Si and B_s atoms in *a*-Si, shown in Fig. 1, are very similar. Indeed, they have the same average bond angle as in *c*-Si. Since by definition, a B_s atom occupies a Si position of the underlying network, it seems that their behavior is structurally similar in *c*- and *a*-Si: they shrink bond

lengths in the same proportion and adopt the angle distribution of the lattice where they are placed. Regarding B_i atoms in a -Si, they have a wider distribution for both bond angles and lengths, which indicates a great variety of different configurations.

The chemical potential of B atoms, μ_B , is calculated as

$$\mu_B = E_{\text{tot}}(a\text{-Si}_n\text{B}) - nE_{\text{tot}}(a\text{-Si}_{64})/64, \quad (1)$$

where n indicates the number of Si atoms in the cell, 63 for B_s and 64 for B_i (in our case, $E_{\text{tot}}(a\text{-Si}_{64})/64 = -5.25$ eV). Figure 2 shows the B chemical potential as a function of the average bond length between the B atom and its nearest neighbors. 62.5% of B_s configurations are inside the limits marked by the straight dashed lines. The solid line corresponds to a linear fit of these configurations. Figure 2 shows that there is more scattering in the data for B_i than for B_s . Chemical potential values scatter within an interval of ~ 1.4 eV for B_s and ~ 3 eV for B_i . However, B_s configurations within the dashed lines represent a linear trend: the longer the average bond, the higher the chemical potential. This linear trend appears to be a lower limit to almost all B_i configurations, which in general have higher energies. Figure 2 also shows that $B_i(4)$ configurations do not display the same trends as B_s and have considerably more scattering.

For charged B atoms in the amorphous cell, the formation energy (E_f) for a system with charge Q as a function of the Fermi level (E_F) is calculated from the expression

$$E_f = E_{\text{tot}}(n, Q) - E_{\text{ref}}(n) + Q(E_v + E_F), \quad (2)$$

where $E_{\text{tot}}(Q)$ is the total energy of the charged system, E_{ref} is the neutral reference energy ($E_{\text{ref}}(n) = E_{\text{tot}}(a\text{-Si}_n\text{B}) + nE_{\text{tot}}(a\text{-Si}_{64})/64$ in a 64-atom supercell), E_v is the energy of the top of the valence band, and E_F is the Fermi energy relative to E_v and ranges from 0 to 1.36 eV, which is the scaled theoretical band gap of a -Si according to our simulations. In order to evaluate the variation of energy when adding/removing one electron, we have only considered those cells in which there were no coordination changes during this process. In order to simulate the energy bias of the distribution in a real system, we have evaluated, for the different coordinations of B atoms (fourfold for B_s and three, four and fivefold for B_i), the Boltzmann averaged formation energy at a typical SPER temperature of 650°C,

$$\langle E_f \rangle = \frac{\sum E_f e^{-E_f/k_B T}}{\sum e^{-E_f/k_B T}}. \quad (3)$$

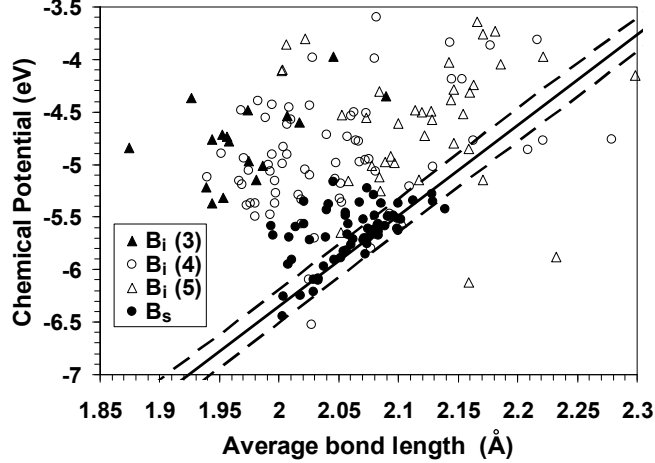


FIG. 2: Chemical potential of B_i and B_s as a function of their average bond length to nearest Si neighbor atoms for the different coordinations. 62.5 % of B_s configurations are inside the limits marked by the dashed lines. The solid line corresponds to a linear fit of these points.

In Fig. 3 we plot the averaged formation energies of B atoms relative to B_s^0 as a function of the Fermi level. Figure. 2(a) shows that B_s^- has a lower energy than both B_s^0 and B_s^+ for the entire Fermi-level range. Therefore, B_s will be negatively charged for all Fermi level values. In the case of B_i , both +1 and -1 charge states can be stable (with a very small stability range for neutral $B_s(3)$). The difference in formation energy between B_s^0 and $B_i^0(4)$ is small. They also have a similar energy dependence on the Fermi level. This suggests that B_s and $B_i(4)$ are similar (substitutional, but with changed a -Si network). The midgap energies correspond in all cases to the negatively charged state, indicating that a -Si will be p -type. Taking the lowest-energy configuration, B_s^- , as reference, they are $E[B_i^-(4)] = 0.30$ eV, $E[B_i^-(5)] = 1.52$ eV, and $E[B_i^-(3)] = 1.54$ eV. Since $B_i(4)$ can be considered as a substitutional-like configuration and $B_i(3)$ and $B_i(5)$ have nearly identical Boltzmann-averaged formation energies, there seems to be a well defined formation energy for interstitial-like B of ~ 1.5 eV at midgap. This result is more than 1 eV smaller than the result of Ref. 9, where possibly, in case numbers and statistics were comparable, just an arithmetic mean has been calculated, which does not take into account the different probabilities of configurations with different energies. Thus, it seems that the amorphous fourfold Si matrix forces B atoms to also have a fourfold-coordinated ground state.

A basic concept of covalent amorphous networks is Mott's "8 - N rule" [20], which asserts that atoms in group I-III take a coordination equal to their valence (thus B would be

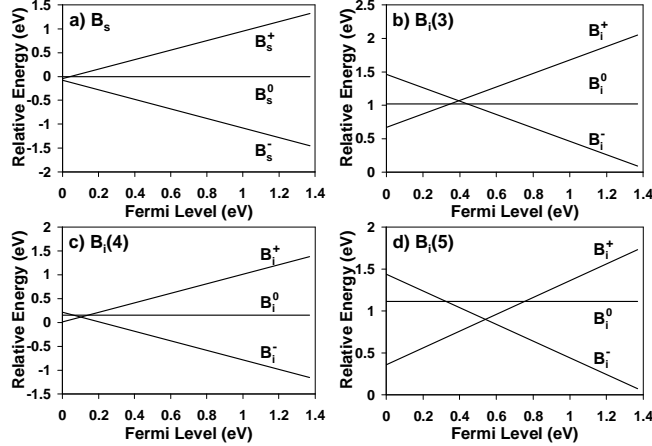


FIG. 3: Formation energies of B_s and B_i relative to B_s^0 as a function of the Fermi level, Boltzmann averaged at 650°C. We have distinguished between B_i atoms with b) three ($B_i(3)$), c) four ($B_i(4)$) and d) five ($B_i(5)$) Si neighbor atoms.

threefold in such a picture). However, this rule seems to be violated in B-doped *a*-Si since the more stable configurations correspond to B_s , explaining the surprising finding that *a*-Si can be doped in agreement with experimental observation [21].

As concerning diffusion, especially in analogy to diffusion in *c*-Si [3], high energy 3 and 5-fold B atoms may be the starting configurations for migration hops. In order to analyze the dynamical features of B in *a*-Si, we have used several B_i and B_s high energy configurations as the starting point of ab initio MD simulations at 1000 K. None of the MD simulations of B_s configurations showed any migration of the B atom within the simulated time of 55 ps. However, frequent local rearrangements of Si-Si bonds occurred. This is very different from Ref. 9 where no major structural changes were observed during MD simulations at an even higher temperature of 1173 K, which led the authors to introducing self-interstitials with different geometry and studying their influence on B diffusion. On the other hand, we could observe a diffusion event in a MD run starting from a $B_i(3)$ configuration. Regarding the diffusion event we observed, we used the Nudged-elastic Band (NEB) method [22] implemented into VASP in order to obtain the energy barriers along the path. Figure 4 shows the nudged-elastic band total energy along the reaction coordinate together with some snapshots of the B environment at the marked points. The highest forward barrier, which represents the overall migration energy from initial to final configuration, is ~ 0.6 eV (similar to the value for *c*-Si [3]). Intermediate forward barriers range from ~ 0.3 to ~ 0.6 eV and may indicate a possible range for migration barriers. The highest reverse

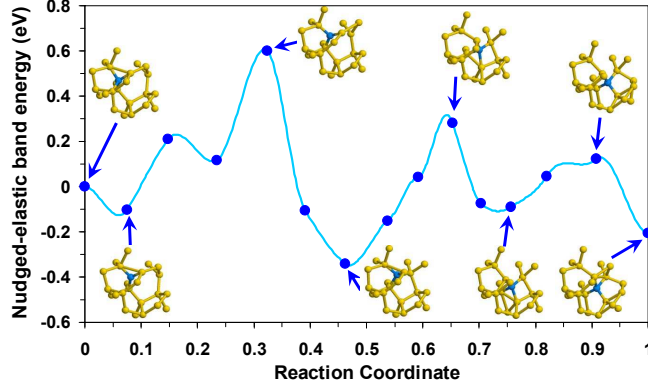


FIG. 4: (Color online) NEB total energy along the diffusion path found, relative to the energy of the initial configuration. Snapshots show the B environment at the indicated points. The B atom is blue (dark), Si atoms are yellow (light).

barrier measures ~ 0.9 eV. It can be seen from the snapshots that in some cases the barriers correspond to Si rearrangement. These rearrangements of the amorphous structure at high temperatures could drag B atoms along. Nevertheless, if B_i is assumed to be the starting point for diffusion, and all the B_i configurations are assumed to have the same migration energy barrier of ~ 0.6 eV, this would result in an activation energy of 2.1 eV, which is in good agreement with experimental observations [23].

Strong B diffusion has been reported during *ab initio* MD simulations of 2 ps at a higher temperature of 1173 K [9]. Assuming the migration barrier reported of 0.7 eV and a typical hopping prefactor of 10^{13} s^{-1} , the average time to observe one B diffusion hop at 1173 K would be $t = 10^{-13} \exp(0.7\text{eV}/k_B T) \sim 100$ ps, considerably longer than 2 ps. Therefore, the events observed may be the initial relaxation of the cell to accommodate the extra atom rather than diffusion.

In summary, we have carried out an *ab initio* study of B in *a*-Si. The structural characterization of B_s atoms indicates that they decrease bonds lengths and acquire the bond angle distribution of the underlying network in a similar way as it happens in *c*-Si. From the analysis of the chemical potential we found that most of the B_s configurations display a linear trend between the averaged B-Si bond length and the chemical potential. No such relationship could be found for B_i , where the energies scattered over a wide range of 3 eV and also overlapped with the energy spread of B_s . High energy configurations of B_i , which correspond to three and five-fold B atoms, are promising candidates to perform diffusion

events. The formation energy of B atoms as a function of the Fermi level confirms the fact that *a*-Si can be doped since fourfold B atoms have the lower energies at mid-gap. B_i has a Boltzmann-averaged formation energy of 1.5 eV with respect to B_s . Finally, from our study of diffusion we have estimated a migration barrier of ~ 0.6 eV. However, contrary to previous findings, dynamics of the underlying Si network can not be separated from the B migration and influence the diffusion event. Despite of that, we could estimate a value of 2.1 eV for the activation energy in good agreement with experiments.

This project has been partially funded by the Ohio Supercomputer Center (computer time); the Spanish DGI under project number TEC2008-0609 (IS, LP, and LAM); the University of Valladolid through the 'Plan de Movilidad del Personal Investigador' (IS); the ARO under MURI W91NF-06-2-0026 (DAD); and the Ohio State University Center for Emergent Materials (a NSF MRSEC; DMR-0820414) (WW).

* Electronic address: `ivasan@tel.uva.es`

† Electronic address: `windl.1@osu.edu`

- [1] N. E. B. Cowern et al., Phys. Rev. Lett. **65**, 2434 (1990); N. E. B. Cowern et al., Phys. Rev. Lett. **67**, 212 (1991).
- [2] B. Sadigh et al., Phys. Rev. Lett. **83**, 4341 (1999).
- [3] W. Windl et al., Phys. Rev. Lett. **83**, 4345 (1999).
- [4] W. Windl, Appl. Phys. Lett. **92**, 202104 (2008).
- [5] X. Y. Liu, W. Windl, and M. P. Masquelier, Appl. Phys. Lett. **77**, 2018 (2000).
- [6] W. Luo et al., J. Appl. Phys. **84**, 2476 (1998).
- [7] L. Pelaz et al., Appl. Phys. Lett. **74**, 3657 (1999).
- [8] P. A. Fedders and D. A. Drabold, Phys. Rev. B **56**, 1864 (1997).
- [9] N. Kong et al., Appl. Phys. Lett. **93**, 082109 (2008).
- [10] International Technology Roadmap for Semiconductors, <http://public.itrs.net>.
- [11] F. Wooten, K. Woner, and D. Weaire, Phys. Rev. Lett. **54**, 1392 (1985).
- [12] N. Mousseau and G. T. Barkema, Phys. Rev. B **61**, 1898 (2000).
- [13] G. T. Barquema and N. Mousseau, Phys. Rev. B **62**, 4895 (2000).
- [14] G. Kresse and J. Hafner, Phys. Rev. B **49**, 14251 (1994); G. Kresse and J. Furthmüller,

- Comput. Mater. Sci. **6**, 15 (1996); G. Kresse and J. Furthmüller, Phys. Rev. B **54**, 11169 (1996).
- [15] J. P. Perdew and Y. Wang, Phys. Rev. B **45**, 13244 (1992).
- [16] W. Windl, Phys. Stat. Sol. B **241**, 2313 (2004).
- [17] S. M. Sze, *The Physics of Semiconductor Devices*, (Wiley, New York, 1969).
- [18] J. S. Lannin, L. J. Pilione, and S. T. Kshirsagar, Phys. Rev. B **26**, 3506 (1982).
- [19] C. Rotaru, S. Nastase, and N. Tomozeiu, Phys. Stat. Sol. A **171**, 365 (1999).
- [20] N. F. Mott, Adv. Phys. **16**, 49 (1967).
- [21] R. A. Street, Phys. Rev. Lett. **49**, 1187 (1982).
- [22] G. Henkelman, B. P. Uberuaga, and H. Jonsson, J. Chem. Phys. **113**, 9901 (2000).
- [23] V. C. Venezia et al., Mat. Sci. and Eng. B **124-125**, 245 (2005).